



New hydrophilic 3-hydroxy-4-pyridinone chelators with ether-derived substituents: Synthesis and evaluation of analytical performance in the determination of iron in waters

Tânia Moniz^{a,*}, Luís Cunha-Silva^a, Raquel B.R. Mesquita^b, Joana L.A. Miranda^b, André M.N. Silva^a, Ana M.G. Silva^a, António O.S.S. Rangel^b, Baltazar de Castro^a, Maria Rangel^{c,*}

^a REQUIMTE-LAQV, Departamento de Química e Bioquímica, Faculdade de Ciências, Universidade do Porto, 4169-007 Porto, Portugal

^b Universidade Católica Portuguesa, CBQF – Centro de Biotecnologia e Química Fina – Laboratório Associado, Escola Superior de Biotecnologia, Rua Arquiteto Lobão Vital 172, 4200-374 Porto, Portugal

^c REQUIMTE-LAQV, Instituto de Ciências Biomédicas de Abel Salazar, Universidade do Porto, 4050-313 Porto, Portugal

ARTICLE INFO

Article history:

Received 16 November 2018

Accepted 7 December 2018

Available online 24 December 2018

Keywords:

3-Hydroxy-4-pyridinone

Iron chelator

Microwave assisted synthesis

X-ray diffraction

Sequential injection

ABSTRACT

Three new hydrophilic 3-hydroxy-4-pyridinone chelators containing ether-derived substituents were prepared by a more sustainable synthetic protocol that involves the use of microwave heating and commercially available amines, allowing the successful production of highly water soluble chelators with improved reaction yields and reaction times. Compared with parent 3-hydroxy-4-pyridinone ligands, the new compounds were obtained faster and in higher amounts, facilitating the scale up of the synthesis, which is crucial to produce these ligands and their respective iron(III) complexes for many biological, analytical and agricultural applications. Ligands were fully characterized by ¹H and ¹³C Nuclear Magnetic Resonance, High Resolution Mass Spectrometry and Single Crystal X-ray Diffraction and their performance in the analytical determination of iron(III) in water samples was evaluated by sequential injection methods. The results obtained are scientifically relevant, pointing out the potential of the new and straightforwardly synthesized ligands as analytical reagents for determination of iron(III).

© 2018 Elsevier Ltd. All rights reserved.

1. Introduction

Hydroxypyridinones are *N*-heterocyclic chelators containing two vicinal oxygen atoms belonging to carbonyl and hydroxyl groups, which confer high affinity towards M^{II}/M^{III} metal ions. Among other hydroxypyridinones, namely 1-hydroxy-2-pyridinone and 3-hydroxy-2-pyridinone, 3-hydroxy-4-pyridinones (3,4-HPOs) are the most studied type of ligands [1,2]. In the last decades, the chemistry and applications of 3,4-HPO have been a central topic of research in the groups of Hider [3–8], Santos [1,9] and Rangel [10–17] thus providing a good number of ligands and complexes that found application in biomedical, analytical, environmental and agriculture applications.

3,4-HPOs are synthetically versatile allowing functionalization by introduction of different substituents in several positions of

the heterocyclic ring, providing chelators with different denticity, physicochemical properties, namely the spectroscopic properties, charge and hydro-lipophilic balance (HLB), without changing their chelating capacity [18–21]. Accordingly, 3,4-HPO have been conjugated with different moieties such as fluorophores [14,22,23], photosensitizers agents for photodynamic therapy [24,25], aminoacids [26] and glycosyl units [27] to be applied in many different fields.

Regarding analytical applications, 3,4-HPO ligands can be used as greener alternative reagents in colorimetric methods for determination of iron in natural waters. This is a topic of great interest since conventional reagents may display high toxicity [28]. Additionally, in the environmental context, the total iron content is not as significant as the free ionic iron content, so methods like Inductively Coupled Plasma Mass Spectrometry (ICP-MS) and Atomic Absorption Spectroscopy (AAS) are not as useful as the spectrophotometric determinations. Monitoring the iron content in natural waters is important due to its impact in esthetic aspects in water, namely color, and also to possible effects in structures deployed in the water bodies.

N-Alkyl-3-hydroxy-4-pyridinones, described in this work as “first generation chelators for analytical purposes” (Fig. 1), have

* Corresponding authors at: Faculdade de Ciências, Universidade do Porto, 4169-007 Porto, Portugal (T. Moniz). Instituto de Ciências Biomédicas de Abel Salazar, Universidade do Porto, 4050-313 Porto, Portugal (M. Rangel).

E-mail addresses: tania.moniz@fc.up.pt (T. Moniz), mrangel@icbas.up.pt, mcran-gel@fc.up.pt (M. Rangel).

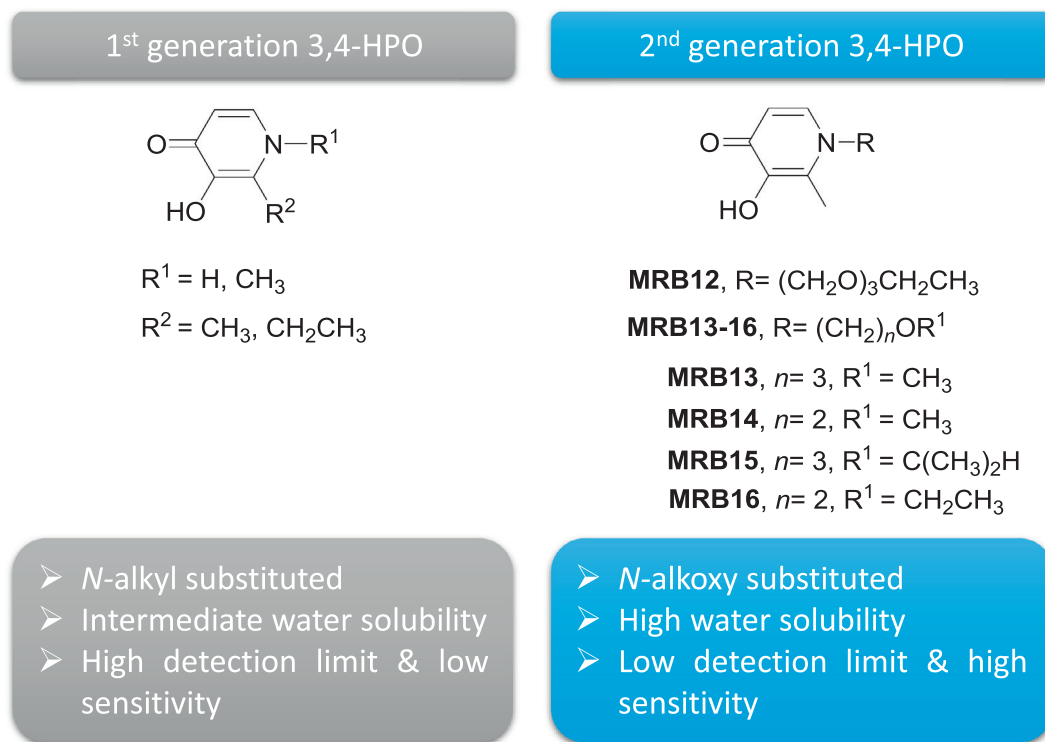


Fig. 1. Numbering and formulae of first and second generation 3,4-HPO used for analytical determination of iron in water samples.

been tested and successfully used for the spectrophotometric sequential injection determination of iron in waters [29,30], although we found that the analytical performance is hampered by ligand's solubility in aqueous media. In line with this fact, a new 3,4-HPO ligand (**PEG-HPO** or **MRB12** [12]) functionalized with a hydrophilic ethylene glycol chain to improve its solubility in water was designed and designated as “second generation 3,4-HPO analytical applications” (Fig. 1). Both the ligand and its iron (III) complex proved to be highly soluble in water providing a lower detection limit and higher sensitivity in flow-based methods for iron determination in water samples [11,12]. As a disadvantage, we found that the synthesis of **MRB12** is costly and poorly efficient presenting numerous reaction steps and a low reaction yield.

In our point of view, the vast number of applications of 3,4-HPO chelators and in particular their promising analytical performance justifies an effort to improve their preparation by means of more efficient and sustainable synthetic routes. Herein, we report the synthesis of other water soluble “second generation 3,4-HPO ligands” containing ether groups (**MRB13**, **MRB15** and **MRB16**, Fig. 1). The use of microwave-assisted organic chemistry instead of “traditional” reflux in oil-bath [12,15,23], allowed reduction of both the reaction times and the possible formation of secondary products. We considered that the use of simpler ether substituents in the nitrogen atom of the heterocyclic ring could reduce the number of reagents as also the number of synthetic steps and consequently improve the efficiency of the synthetic approach without compromising water solubility and the analytical performance.

The structural characterization of all ligands was achieved by ^1H and ^{13}C Nuclear Magnetic Resonance, High Resolution Mass Spectrometry and Single Crystal X-ray Diffraction.

The 3,4-HPO ligands **MRB13**, **MRB14**, **MRB15** and **MRB16** were investigated regarding their potential use in the analytical determination of iron(III) by sequential injection methods (SI) and results were compared with those reported for **PEG-HPO** or **MRB12** ligand. The assessment of potential interferences of a set

of metal ions in the determination of iron in water samples was also investigated for all the ligands.

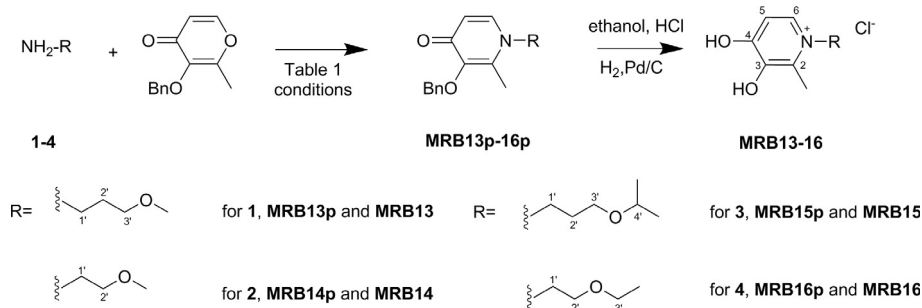
2. Experimental

2.1. Materials and physical measurements

Chemicals were obtained from Sigma–Aldrich (grade puriss, p.a.) or Fluka (p.a.) and were used as received unless otherwise specified. The 3-benzyloxy-2-methyl-4-pyrone (Scheme 1, A) was synthesized in our laboratory following the procedures described in the literature [31].

Microwave-assisted reactions were carried out in a CEM Discovery Labmate circular single-mode cavity instrument (300 W max magnetron power output) from CEM Corporation, using standard Pyrex vessels (capacity 30 mL) under sealed vessel conditions. NMR spectra were recorded on a Bruker Avance III 400 spectrometer, operating at 400.15 MHz for ^1H and 100.62 MHz for ^{13}C atoms, equipped with pulse gradient units, capable of producing magnetic field pulsed gradients in the z-direction of 50.0 G/cm. Two-dimensional $^1\text{H}/^1\text{H}$ correlation spectra (COSY), gradient selected $^1\text{H}/^{13}\text{C}$ heteronuclear single quantum coherence (HSQC) and $^1\text{H}/^{13}\text{C}$ heteronuclear multiple bond coherence (HMBC) spectra were acquired using the standard Bruker software.

High resolution electrospray ionization mass spectra (ESI-MS) were obtained in a Thermo Scientific LTQ-Orbitrap XL mass spectrometer, externally calibrated with a standard kit provided by the manufacturer. The spectrometer was operated in the positive ionization mode setting the capillary voltage to +3.0 kV, sheath gas flow to 6 and the temperature of the ion transfer capillary to 275 °C. Spectra were recorded for m/z values between 250 and 2000 in the Fourier Transform (FT) mode with resolution (FWHM) set at 60 000. Samples were prepared in water, diluted in a 50% (v/v) water:methanol mixture immediately before analysis and



Scheme 1. General approach to access *N*-alkoxy substituted 3-hydroxy-4-pyridinones.

directly infused into the electrospray ion source utilizing the syringe pump in the mass spectrometer at $10 \mu\text{L min}^{-1}$. NMR and Mass spectrometry analyses were performed at Laboratório de Análise Estrutural, Centro de Materiais da Universidade do Porto (CEMUP) (Portugal).

2.2. Synthesis of protected 3,4-HPO ligands

2.2.1. Synthesis of 1-(3'-methoxypropyl)-2-methyl-3-benzyloxy-4-(1H)-pyridinone (**MRB13p**)

A mixture of amine **1** (3-methoxypropylamine) (2.086 g, 0.0234 mol) and protected pyrone (3-benzyloxy-2-methyl-4-pyrone) (0.505 g, 0.0023 mol) dissolved in dried ethanol (2 mL) was placed in a 30 mL reaction vial, which was then closed under argon atmosphere and placed in the cavity of a CEM microwave reactor. The reaction vial was irradiated to 80°C during 4 h, using 100 W maximum power. The reaction solvent was evaporated and the crude oil resultant was dissolved in 30 mL of H_2O and the pH adjusted to 1 with HCl 10%. The starting materials were removed by liquid/liquid extraction with diethyl ether. The organic layer was rejected. The pH of aqueous phase was adjusted to 10 with a solution of NaOH 5% and the product was then extracted to the organic layer with dichloromethane. The organic phase was concentrated to afford compound **MRB13p** (0.620 g, 92% yield) as dark brown oil.

400.15 MHz ^1H NMR (CDCl_3 , ppm): δ 1.83 (m, 2H, H_2'), 2.09 (s, 3H, 2- CH_3), 3.26 (t, J 5.6 Hz, 2H, H_3'), 3.29 (s, 3H, $-\text{OCH}_3$), 3.88 (t, J 7.0 Hz, 2H, H_1'), 5.19 (s, 2H, $-\text{CH}_2\text{C}_6\text{H}_5$), 6.41 (d, J 7.5 Hz, 1H, H_5), 7.24 (d, J 7.5 Hz, 1H, H_6), 7.29–7.32 (m, 3H, $\text{H}_{\text{meta+para}}-\text{CH}_2\text{C}_6\text{H}_5$), 7.38–7.40 (m, 2H, $\text{H}_{\text{ortho}}-\text{CH}_2\text{C}_6\text{H}_5$). 100.62 MHz ^{13}C NMR (CDCl_3 , ppm): δ 12.2 (2- CH_3), 30.3 (C_2'), 50.4 (C_1'), 58.6 ($-\text{OCH}_3$), 67.8 (C_3'), 72.9 ($-\text{CH}_2\text{C}_6\text{H}_5$), 117.0 (C5), 127.9 and 128.2 ($\text{C}_{\text{meta+para}}-\text{C}_6\text{H}_5$), 129.0 ($\text{C}_{\text{ortho}}-\text{C}_6\text{H}_5$), 137.5 (Cq, $-\text{C}_6\text{H}_5$), 138.6 (C6), 141.1 (C2), 145.9 (C3), 173.2 (C4).

2.2.2. Synthesis of 1-(2'-methoxyethyl)-2-methyl-3-benzyloxy-4-(1H)-pyridinone (**MRB14p**)

A mixture of amine **2** (2-methoxyethylamine) (0.691 g, 0.00928 mol) and protected pyrone (3-benzyloxy-2-methyl-4-pyrone) (0.501 g, 0.00232 mol) dissolved in dried ethanol (2 mL) was placed in a 30 mL reaction vial, which was then closed under argon atmosphere and placed in the cavity of a CEM microwave reactor. The reaction vial was irradiated to 90°C during 4 h, using 100 W maximum power. The reaction solvent was evaporated and the crude oil resultant was dissolved in 30 mL of H_2O and the pH adjusted to 1 with HCl 10%. The starting materials were removed by liquid/liquid extraction with diethyl ether. The organic layer was rejected. The pH of aqueous phase was adjusted to 10 with a solution of NaOH 5% and the product was then extracted to the organic layer with dichloromethane. The organic phase was con-

centrated to afford compound **MRB14p** (0.434 g, 69% yield) as dark brown oil.

400.15 MHz ^1H NMR (CDCl_3 , ppm): δ 2.10 (s, 3H, 2- CH_3), 3.24 (s, 3H, $-\text{OCH}_3$), 3.49 (t, J 5.0 Hz, 2H, H_2'), 3.92 (t, J 5.0 Hz, 2H, H_1'), 5.15 (s, 2H, $-\text{CH}_2\text{C}_6\text{H}_5$), 6.37 (d, J 7.5 Hz, 1H, H_5), 7.28–7.30 (m, 1H, H_6 and 3H, $\text{H}_{\text{meta+para}}-\text{CH}_2\text{C}_6\text{H}_5$), 7.38–7.40 (m, 2H, $\text{H}_{\text{ortho}}-\text{CH}_2\text{C}_6\text{H}_5$). 100.62 MHz ^{13}C NMR (CDCl_3 , ppm): δ 12.3 (2- CH_3), 52.8 (C_1'), 58.8 ($-\text{OCH}_3$), 70.9 (C_2'), 72.6 ($-\text{CH}_2\text{C}_6\text{H}_5$), 116.4 (C5), 127.6 and 127.9 ($\text{C}_{\text{meta+para}}-\text{C}_6\text{H}_5$), 128.7 ($\text{C}_{\text{ortho}}-\text{C}_6\text{H}_5$), 137.2 (Cq, $-\text{C}_6\text{H}_5$), 139.0 (C6), 141.3 (C2), 145.4 (C3), 173.0 (C4).

2.2.3. Synthesis of 1-(3'-isopropoxypropyl)-2-methyl-3-benzyloxy-4-(1H)-pyridinone (**MRB15p**)

A mixture of amine **3** (3-isopropoxypropylamine) (1.645 g, 0.0141 mol) and protected pyrone (3-benzyloxy-2-methyl-4-pyrone) (0.507 g, 0.0024 mol) dissolved in dried ethanol (2 mL) was placed in a 30 mL reaction vial, which was then closed under argon atmosphere and placed in the cavity of a CEM microwave reactor. The reaction vial was irradiated to 80°C during 4 h, using 100 W maximum power. The reaction solvent was evaporated and the crude oil resultant was dissolved in 30 mL of H_2O and the pH adjusted to 1 with HCl 10%. The starting materials were removed by liquid/liquid extraction with diethyl ether. The organic layer was rejected. The pH of aqueous phase was adjusted to 10 with a solution of NaOH 5% and the product was then extracted to the organic layer with dichloromethane. The organic phase was concentrated to afford compound **MRB15p** (0.565 g, 89% yield) as dark brown oil.

400.15 MHz ^1H NMR (CDCl_3 , ppm): δ 1.14 (d, J 6.3 Hz, 6H, $4'-(\text{CH}_3)_2$), 1.83 (quint, J 6.2 Hz, 2H, H_2'), 2.11 (s, 3H, 2- CH_3), 3.30 (t, J 5.4 Hz, 2H, H_3'), 3.51 (m, J 6.3 Hz, 1H, $4'-\text{CH}$), 3.89 (t, J 7.0 Hz, 2H, H_1'), 5.24 (s, 2H, $-\text{CH}_2\text{C}_6\text{H}_5$), 6.40 (d, J 7.6 Hz, 1H, H_5), 7.22 (d, J 7.6 Hz, 1H, H_6), 7.28–7.42 (m, 5H, $\text{CH}_2\text{C}_6\text{H}_5$). 100.62 MHz ^{13}C NMR (CDCl_3 , ppm): δ 12.3 (2- CH_3), 22.0 ($4'-(\text{CH}_3)_2$), 30.8 (C_2'), 50.5 (C_1'), 63.1 (C_3'), 71.9 (C_4'), 72.9 ($-\text{CH}_2\text{C}_6\text{H}_5$), 117.2 (C5), 127.9 and 128.2 and 129.2 ($-\text{C}_6\text{H}_5$), 137.7 (Cq, $-\text{C}_6\text{H}_5$), 138.5 (C6), 140.7 (C2), 146.1 (C3), 173.4 (C4).

2.2.4. Synthesis of 1-(2'-ethoxyethyl)-2-methyl-3-benzyloxy-4-(1H)-pyridinone (**MRB16p**)

A mixture of amine **4** (2-ethoxyethylamine) (0.825 g, 0.0092 mol) and protected pyrone (3-benzyloxy-2-methyl-4-pyrone) (0.500 g, 0.00231 mol) dissolved in dried ethanol (2 mL) was placed in a 30 mL reaction vial, which was then closed under argon atmosphere and placed in the cavity of a CEM microwave reactor. The reaction vial was irradiated to 80°C during 5 h, using 100 W maximum power. The reaction solvent was evaporated and the crude oil resultant was dissolved in 30 mL of H_2O and the pH adjusted to 1 with HCl 10%. The starting materials were removed by liquid/liquid extraction with diethyl ether. The organic layer was rejected. The pH of aqueous phase was adjusted to 10 with a

solution of NaOH 5% and the product was then extracted to the organic layer with dichloromethane. The organic phase was concentrated to afford compound **MRB16p** (0.576, 91% yield) as dark brown oil.

400.15 MHz ^1H NMR (CDCl_3 , ppm): δ 1.11 (t, J 7.0 Hz, 3H, 3'-CH₃), 2.11 (s, 3H, 2-CH₃), 3.39 (q, J 7.0 Hz, 2H, H3'), 3.55 (t, J 5.0 Hz, 2H, H2'), 3.92 (t, J 5.0 Hz, 2H, H1'), 5.19 (s, 2H, —CH₂C₆H₅), 6.39 (d, J 7.8 Hz, 1H, H5), 7.26 (d, J 7.8 Hz, 1H, H6), 7.30–7.42 (m, 5H, CH₂C₆H₅). 100.62 MHz ^{13}C NMR (CDCl_3 , ppm): δ 12.7 (2-CH₃), 15.0 (3'-CH₃), 53.3 (C1'), 67.0 (C3'), 69.1 (C2'), 73.0 (—CH₂C₆H₅), 116.9 (C5), 127.9 and 128.2 and 129.0 (—C₆H₅), 137.6 (Cq, —C₆H₅), 139.1 (C6), 141.1 (C2), 145.8 (C3), 173.5 (C4).

2.2.5. Removal of benzyl protecting group of 3,4-HPO ligands

Each protected 3,4-HPO: **MRB13p** (0.620 g, 0.0022 mol), **MRB14p** (0.434 g, 0.0016 mol), **MRB15p** (0.565 g, 0.0018 mol) and **MRB16p** (0.576 g, 0.0020 mol) was dissolved in ethanol (20 mL) and HCl (20 μL) and placed into a hydrogenation vessel. The air was removed with N₂, a catalytic amount of 10% Pd/C (w/w) was added and the mixture was stirred at room temperature, with H₂ at 40 psi for 6 h. The reaction mixtures were filtered, washed with methanol and chloroform and the solvents were evaporated in vacuum to give a brown oil product. The resulting residues were dried under vacuum to give the hydrochloride salt of each 3,4-HPO: **MRB13** (0.477 g, 95% yield), **MRB14** (0.366 g, 100% yield), **MRB15** (0.457 g, 98% yield) and **MRB16** (0.430, 92% yield).

1-(3'-Methoxypropyl)-2-methyl-3-hydroxy-4-1H-pyridinone hydrochloride (**MRB13**). MS: calculated for C₁₀H₁₆NO₃⁺: 198.1125 (monoisotopic molecular weight M⁺), found: HRMS: 198.1121. 400.15 MHz ^1H NMR (MeOD-*d*₄, ppm): δ 2.11 (quint, J 6.7 Hz, 2H, H2'), 2.65 (s, 3H, 2-CH₃), 3.32 (s, 3H, —OCH₃), 3.43 (t, J 5.6 Hz, 2H, H3'), 4.48 (t, J 7.3 Hz, 2H, H1'), 7.12 (d, J 6.9 Hz, 1H, H5), 8.13 (d, J 6.9 Hz, 1H, H6). 100.62 MHz ^{13}C NMR (MeOD-*d*₄, ppm): δ 12.7 (2-CH₃), 31.1 (C2'), 55.4 (C1'), 59.0 (—OCH₃), 69.5 (C3'), 111.8 (C5), 139.5 (C6), 143.7 (C2), 145.1 (C3), 159.8 (C4).

1-(2'-Methoxyethyl)-2-methyl-3-hydroxy-4-(1H)-pyridinone hydrochloride (**MRB14**). MS: calculated for C₉H₁₄NO₃⁺: 184.0968 (monoisotopic molecular weight M⁺), found: HRMS: 184.0969. 400.15 MHz ^1H NMR (MeOD-*d*₄, ppm): δ 2.64 (s, 3H, 2-CH₃), 3.31 (s, 3H, —OCH₃), 3.78 (t, J 4.7 Hz, 2H, H2'), 4.59 (t, J 4.7 Hz, 2H, H1'), 7.16 (d, J 6.8 Hz, 1H, H5), 8.14 (d, J 6.8 Hz, 1H, H6). 100.62 MHz ^{13}C NMR (MeOD-*d*₄, ppm): δ 13.2 (2-CH₃), 57.2 (C1'), 59.4 (—OCH₃), 71.6 (C2'), 111.4 (C5), 140.0 (C6), 143.9 (C2), 144.7 (C3), 159.7 (C4).

1-(3'-Isopropoxypropyl)-2-methyl-3-hydroxy-4-(1H)-pyridinone hydrochloride (**MRB15**). MS: calculated for C₁₂H₂₀NO₃⁺: 226.1438 (monoisotopic molecular weight M⁺), found: HRMS: 226.1442. 400.15 MHz ^1H NMR (MeOD-*d*₄, ppm): δ 1.12 (d, J 6.3 Hz, 6H, 4'-(CH₃)₂), 2.10 (quint, J 6.4 Hz, 2H, H2'), 2.66 (s, 3H, 2-CH₃), 3.49 (t, J 5.6 Hz, 2H, H3'), 3.57 (m, J 6.3 Hz, 1H, 4'-CH), 4.48 (t, J 7.0 Hz, 2H, H1'), 7.10 (d, J 7.0 Hz, 1H, H5), 8.13 (d, J 7.0 Hz, 1H, H6). 100.62 MHz ^{13}C NMR (MeOD-*d*₄, ppm): δ 12.8 (2-CH₃), 22.3 (4'-(CH₃)₂), 31.5 (C2'), 55.6 (C1'), 65.0 (C3'), 73.1 (C4'), 111.6 (C5), 139.4 (C6), 143.6 (C2), 145.1 (C3), 159.6 (C4).

1-(2'-Ethoxyethyl)-2-methyl-3-hydroxy-4-(1H)-pyridinone hydrochloride (**MRB16**). MS: calculated for C₁₀H₁₆NO₃⁺: 198.1125 (monoisotopic molecular weight M⁺), found: HRMS: 198.1125. 400.15 MHz ^1H NMR (MeOD-*d*₄, ppm): δ 1.10 (t, J 7.0 Hz, 3H, 3'-CH₃), 2.67 (s, 3H, 2-CH₃), 3.48 (q, J 7.0 Hz, 2H, H3'), 3.85 (t, J 5.0 Hz, 2H, H2'), 4.62 (t, J 5.0 Hz, 2H, H1'), 7.22 (d, J 7.0 Hz, 1H,

H5), 8.19 (d, J 7.0 Hz, 1H, H6). 100.62 MHz ^{13}C NMR (MeOD-*d*₄, ppm): δ 13.3 (2-CH₃), 15.2 (3'-CH₃), 57.3 (C1'), 67.7 (C3'), 69.5 (C2'), 111.4 (C5), 140.0 (C6), 143.9 (C2), 144.5 (C3), 159.7 (C4).

2.3. Single-crystal X-ray diffraction

Suitable single crystals of the compounds **MRB13**–**MRB16** were manually harvested and a mounted on cryoloops using viscous FOMBLIN Y perfluoropolyether vacuum oil (LVAC 140/13, Sigma-Aldrich) [32]. Diffraction data were collected at on a Bruker X8 Kappa APEX II Charge-Coupled Device (CCD) area-detector diffractometer controlled by the APEX2 software package [33] (Mo K α graphite-monochromated radiation, λ = 0.71073 Å), and equipped with an Oxford Cryosystems Series 700 cryostream monitored remotely with the software interface Cryopad (acquisition temperature of 150.0(2) K) [34]. Images were processed with the software SAINT+ [35], and the absorption effects were corrected by the multi-scan method implemented in SADABS [36]. The structures were solved using SHELXT-2014 [37,38], which allow the immediate location and identification of a considerable number of the heaviest atoms composing the asymmetric unit. The remaining absent and misplaced non-hydrogen atoms were located from difference Fourier maps from successive full-matrix least-squares refinement cycles on F^2 using SHELXL-v.2014 [37,39]. All the non-hydrogen atoms were successfully refined using anisotropic displacement parameters.

Hydrogen atoms bonded to carbon were placed at their geometrical positions using the appropriate HFIX instructions (137 for the terminal —CH₃, 23 for the —CH₂— and 43 for the aromatic groups) and included in subsequent refinement cycles in riding-motion approximation with isotropic thermal displacements parameters (U_{iso}) fixed at 1.2 or 1.5 $\times U_{\text{eq}}$ of the relative atom. Furthermore, the hydrogen atoms associated to hydroxyl groups and the crystallization water molecule (only in the **MRB16** structure) were markedly visible in the difference Fourier maps and included in subsequent refinement stages with the O—H distances restrained to 0.90(2), and using a riding-motion approximation with an isotropic thermal displacement parameter fixed at 1.5 $\times U_{\text{eq}}$ of the oxygen atom.

Information concerning the crystallographic data collection and structure refinement details is summarized in Table 1, while the geometrical details about the strong hydrogen bonding interactions are shown in Table 4.

2.4. Analytical procedure for iron(III) quantification

2.4.1. Reagents and solutions

Ligand stock solutions were obtained by dissolving circa 20 mg of each ligand in 2.0 mL of Milli-Q water (MQW), corresponding to an approximate concentration of about 42 mmol/L. Working ligand solutions were obtained by dilution of the stock solutions to final concentration of about 0.6 mmol/L.

A 0.25 mol/L hydrogen carbonate buffer solution was prepared by dissolving 1.05 g of sodium hydrogen carbonate (Merck, Germany) in 50 mL of water and adjusting the pH to 10.6 with 0.5 mol/L sodium hydroxide solution. A solution of 0.5 M nitric acid was prepared from dilution of the concentrated acid (d = 1.4; 65%, Merck, Germany).

An iron(III) stock solution of 10 mg/L (180 μM) was obtained by dilution of the atomic absorption standard (1001 mg/L Fluka – Sigma-Aldrich, Switzerland). This solution was used to prepare the Fe³⁺ working standards in the dynamic range 0.1–1.0 mg/L (1.8–18 $\mu\text{mol/L}$) in 0.03 M nitric acid.

Table 1Crystal and structure refinement data for compounds **MRB13**–**MRB16**.

	MRB13	MRB14	MRB15	MRB16
Formula	C ₁₀ H ₁₆ ClNO ₃	C ₉ H ₁₄ ClNO ₃	C ₁₂ H ₂₀ ClNO ₃	C ₁₀ H ₁₈ ClNO ₄
<i>Mr</i>	233.69	219.66	261.74	251.70
Crystal morphology	colorless block	colorless prism	colorless block	colorless prism
Crystal size (mm)	0.12 × 0.04 × 0.03	0.19 × 0.15 × 0.11	0.14 × 0.09 × 0.06	0.20 × 0.03 × 0.02
Crystal system	monoclinic	orthorhombic	monoclinic	monoclinic
Space group	<i>P</i> 2 ₁ / <i>c</i>	<i>P</i> 2 ₁ 2 ₁ 2 ₁	<i>P</i> 2 ₁ / <i>c</i>	<i>P</i> 2 ₁ / <i>c</i>
<i>Unit cell dimensions</i>				
<i>a</i> (Å)	7.768(2)	7.087(7)	11.9647(15)	7.5041(7)
<i>b</i> (Å)	13.119(3)	11.804(11)	8.6675(11)	13.1185(12)
<i>c</i> (Å)	11.731(3)	12.141(11)	13.3471(19)	12.6117(12)
α (°)	90	90	90	90
β (°)	108.919(10)	90	106.863(6)	93.190(4)
γ (°)	90	90	90	90
<i>V</i> (Å ³)	1131.0(5)	1015.6(2)	1324.6(3)	1239.6(2)
<i>Z</i>	4	4	4	4
ρ_{calc} (g cm ^{−3})	1.372	1.437	1.312	1.349
<i>F</i> (0 0 0)	496	464	560	536
μ (mm ^{−1})	0.325	0.357	0.286	0.308
θ range (°)	3.672–25.677	3.750–27.474	3.947–26.370	3.60–25.025
Index ranges	−9 ≤ <i>h</i> ≤ 9 −15 ≤ <i>k</i> ≤ 15 −14 ≤ <i>l</i> ≤ 11	−8 ≤ <i>h</i> ≤ 9 −15 ≤ <i>k</i> ≤ 15 −15 ≤ <i>l</i> ≤ 15	−13 ≤ <i>h</i> ≤ 14 −10 ≤ <i>k</i> ≤ 10 −16 ≤ <i>l</i> ≤ 16	−8 ≤ <i>h</i> ≤ 8 −15 ≤ <i>k</i> ≤ 15 −14 ≤ <i>l</i> ≤ 14
Reflections collected	8788	8296	15 993	29 379
Independent reflections	2139 (<i>R</i> _{int} = 0.0903)	2317 (<i>R</i> _{int} = 0.0349)	2700 (<i>R</i> _{int} = 0.0606)	2165 (<i>R</i> _{int} = 0.0271)
Final <i>R</i> indices [<i>I</i> > 2σ(<i>I</i>)]	<i>R</i> ₁ = 0.0499; <i>wR</i> ₂ = 0.1008	<i>R</i> ₁ = 0.0277; <i>wR</i> ₂ = 0.0669	<i>R</i> ₁ = 0.0381; <i>wR</i> ₂ = 0.0886	<i>R</i> ₁ = 0.0242; <i>wR</i> ₂ = 0.0630
Final <i>R</i> indices (all data)	<i>R</i> ₁ = 0.0956; <i>wR</i> ₂ = 0.1186	<i>R</i> ₁ = 0.0305; <i>wR</i> ₂ = 0.0690	<i>R</i> ₁ = 0.0593; <i>wR</i> ₂ = 0.0980	<i>R</i> ₁ = 0.0266; <i>wR</i> ₂ = 0.0645
Largest difference peak and hole (e Å ^{−3})	0.262 and −0.318	0.202 and −0.184	0.305 and −0.202	0.216 and −0.157

2.4.2. Analytical flow analysis procedure

The analytical procedure to test the different ligands as colorimetric reagent for iron(III) determination has been previously described [12]. The micro sequential injection system comprised a MicroSIA of FIALab (FIALab Instruments, USA), consisting in a bi-directional syringe pump of 2.5 mL and an eight-port selection valve (Valco VICI Cheminert 170-0317L), connected to the central channel of with a PVC pumping tube.

The other system components were connected with PTFE (OmniFit) tubing, with 0.8 mm i.d.

Detection of the colorimetric reaction was attained with an Ocean Optics Flame – T – UV– Vis (FLMT01897) charged coupled device (CCD) detector, equipped with a pair of FIA-P600-Fiber cable 600 Micron diameter (SMA terminated on one end and PEEK sheath termination on the other end), an Ocean Optics halogen light source HL-2000 and a FIA-Z-Cell 100 mm – Plexiglas FIA-Z Cell with adjustable optical path (10 cm light path and 250 µL inner volume). Data acquisition, made at 460 nm, 475 nm and 515 nm. All the equipment was controlled on a desktop computer with FIALab software installed (Lenovo, Intel Core i5).

The protocol sequence used for iron(III) determination has also been previously detailed [12] and consisted in aspirating ligand solution (250 µL), followed by buffer solution (20 µL) and iron standard (500 µL), and then propelling the mixture towards the detector for signal registration.

3. Results and discussion

3.1. Design and synthesis of 3,4-HPOs

The general synthetic approach to prepare a 3-hydroxy-4-pyridinone ligand involves the reaction of a 3-hydroxy-4-pyrone with a primary amine [12,31,40]. The hydroxyl group in the position 3 of the pyrone ring was previously protected with a benzyl group, according with methods previously described [31]. Then,

different –R substituents were introduced by the substitution of the oxygen by the nitrogen atom of the amine leading to 3,4-HPOs with different *N*-chains and variable physicochemical properties. The choice of the amine is determinant for the hydrophilic-lipophilic balance of the new 3,4-HPO ligand. Considering these criteria (discussed below), four alkoxyamines including 3-methoxypropylamine, 2-methoxyethylamine, 3-isopropoxypropylamine and 2-ethoxyethylamine, were selected to react with 3-benzoyloxy-2-methyl-4-pyrone using microwave-assisted synthesis (Scheme 1, Table 2).

The synthesis of ligand **MRB14** was previously reported by Hider and co-workers [41,42] nonetheless in the present work the ligand was obtained by using microwave-assisted synthesis instead of the traditional heating method previously described. The compound **MRB14** was included in the set of molecules considered in the present work as it is structurally related and we are interested in the study of the influence of the chelator's structure for the performance of the ligands and their respective iron (III) complexes in the analytical and biological context, namely as plant fertilizers [17].

The protocol established for the synthesis of **MRB12** includes the preparation of the polyethylene glycol (PEG) functionalized amine thus implying two additional reaction steps, which consti-

Table 2Yields of *N*-alkoxy substituted 3-benzoyloxy-4-pyridinones on microwave heating under closed vessel conditions.^a

<i>N</i> -Alkoxy 3-benzoyloxy-4-pyridinones	Conditions	Amine (excess)	Yield (%)
MRB13p	80 °C, 4 h	10 equiv.	92
MRB14p	90 °C, 4 h	4 equiv.	69
MRB15p	80 °C, 4 h	6 equiv.	89
MRB16p	80 °C, 5 h	4 equiv.	91

^a Reactions of primary amines with 3-benzoyloxy-2-methyl-4-pyrone (0.5 g, 2 mmol) were performed in dried ethanol (2 mL).

tutes a disadvantage. In the present work we chose to use commercially available amines (Scheme 1, 1–4) to produce the new ligands. This alternative allowed the reduction of the numbers of reaction steps from 5 to 3 and significantly decreased the total time of reaction, when compared with the method described for the synthesis of **MRB12** [12]. This choice of amines together with the use of microwave heating instead of “traditional” reflux in oil-bath aimed to contribute to a simpler and more sustainable synthetic protocol for ligand production, mainly by reducing reaction time and improve the reproducibility of the experiments.

The microwave heating process is based on the ability of a material to heat when exposed to an alternating electric field and depends on the dielectric properties of that material (expressed as the loss factor, $\tan \delta$) [43,44]. In fact, the reactions under study were performed in ethanol, which presents a high $\tan \delta$ value ($\tan \delta = 0.941$) [45], meaning that it is a strong microwave absorbing solvent and, in combination with reaction reagents, should provide an efficient absorption and rapid heating profile. The microwave-assisted synthesis of the ligands afforded: (a) **MRB13p**, **MRB15p** and **MRB16p** in good reaction yields in 4 or 5 h (69–92%) (Table 2) and (b) ligand **MRB14p** in a significantly shorten reaction time (4 h) when compared with the “traditional” reflux protocol (18 h) [41], a reduction of approximately 78%, despite maintaining the reaction yield.

In all reactions an excess of amine was used, starting from two-fold excess, although we found that a fourfold excess is required to get ligands **MRB14p** and **MRB16p**. Ligand **MRB15p** required a higher amount of amine and the best results were obtained using six times more amine than the protected pyrone. Amine 1 seems to be the less reactive and a tenfold excess of amine was required to get the **MRB13p**.

Purification of the protected ligands was achieved by liquid–liquid extraction without need of extra purification by chromatography, in opposition with purification of **MRB12p**. This fact may justify the higher yields for **MRB13p**–**MRB16p** contrasting with 49% (**MRB12p**) [12].

In order to obtain the deprotected form of the 3,4-HPO ligand, the benzyl-protecting group was removed under a hydrogen atmosphere in the presence of Pd/C (10%) and HCl, yielding the **MRB13**–**MRB16** ligands hydrochloride salt in almost quantitative (92–100%) yield.

3.2. Selection of amine reagents and prediction of Log P values

Taking into account the objective of this work, the selection of amines was based on the Log P values, predicted using the ACD/Log P Software [46] (Table 3) and commercial availability.

The reaction of the selected amines with the protected 2-methyl-3-hydroxy-4-pyrone originated the new set ligands listed in Table 3 that have log P values in the range –0.50 to 0.50.

Compounds **MRB13** and **MRB14** exhibit Log P values quite similar to that found for PEGylated 3,4-HPO (**MRB12**) [12]. **MRB15** and **MRB16** Log P values are predicted to be slightly more lipophilic than **MRB12**, a property that may be advantageous for different applications.

3.3. NMR spectroscopy

The structures of the protected and deprotected ligands in solution were established by NMR analysis (^1H and ^{13}C , 1D and 2D experiments, including COSY, HSQC and HMBC spectra for unequivocal assignment of the most characteristic proton and carbon chemical shifts). The assignment of the resonance signals in ^{13}C NMR spectra of the protected and deprotected compounds was achieved by analysis of $^1\text{H}/^{13}\text{C}$ HSQC and $^1\text{H}/^{13}\text{C}$ HMBC spectra, which provide one and multiple bond ^1H – ^{13}C connectivity,

respectively. All the chemical shift values obtained are in a good agreement with those described in the literature for similar compounds [12,40]. All spectra are available in supporting information (Figs. S1–S22). As a representative example, the detailed discussion of the ^1H and ^{13}C spectra of compounds **MRB13p** and **MRB13** is described below. For the other ligands synthesized, an extended description of the NMR spectra is available in supporting information.

^1H and ^{13}C spectra of **MRB13p** revealed multiplets in the aliphatic region (1.83, 3.26 and 3.88 ppm) which were assigned to protons of $-\text{CH}_2$ groups ($\text{H}2'$, $\text{H}3'$ and $\text{H}1'$, respectively) of the *N*-substituent and their carbons, $\text{C}2'$, $\text{C}1'$ and $\text{C}3'$, appear at 30.3, 50.4 and 67.8 ppm, respectively. Carbon $\text{C}1'$ exhibited long range HMBC correlation with proton H6, allowing the assignment performed. The resonance signal of the methoxyl protons in the terminal group ($-\text{OCH}_3$) appears at 3.29 ppm and the associated carbon ($-\text{OCH}_3$) appears at 58.6 ppm and shows HSQC correlation. Upon the deprotection (**MRB13**), significant differences in the ^1H and ^{13}C spectra were detected as the shift of the protons closely to the pyridinone ring, namely 2- CH_3 , H5 and H6 protons, in agreement with the results previously described [47]. The most affected signal of the *N*-substituent was $\text{H}1'$ proton which chemical shift varied from 3.88 to 4.48 ppm. In the ^{13}C spectrum, some variations were also verified, namely $\text{C}1'$ carbon which signal shifted from 50.4 to 55.4 ppm. The resonance signal at 31.1 ppm was attributed to $\text{C}2'$ carbon due to its HMBC correlation with $\text{H}1'$ and $\text{H}3'$ protons. $\text{C}1'$ (55.4 ppm) has shown correlation with the signal H6, $\text{H}3'$ and $\text{H}2'$, allowing its attribution.

The observed differences in the chemical shifts of ^1H and ^{13}C nucleus in the spectra of the protected and deprotected forms of each compound are primarily justified by the different solvent used for the NMR studies of protected (CDCl_3) and deprotected forms (MeOD) which as deliberated by the different solubility of each form of the ligand. Moreover, the deprotection of the hydroxyl group in acidic reaction conditions leads to isolate the final ligands in the enolic form, thus justifying the variations of the chemical shifts of the protons and carbons signals [47].

3.4. Solid-state structures

Crystalline material of the four 3,4-HPO ligands (**MRB13**–**MRB16**) revealing single-crystals suitable for X-ray diffraction analysis were obtained by controlled recrystallization from MeOH/ CHCl_3 solvent mixtures. The solid-state crystalline structures were solved and determined in the monoclinic space group $P2_1/c$, with the exception of **MRB14** for which crystallized in the orthorhombic system (space group $P2_12_12_1$).

The crystal structure of ligand **MRB14** was firstly reported by Hider and co-workers [42]. As it was possible to obtain crystalline material of **MRB14** revealing single-crystals suitable for X-ray diffraction analysis, we also included the description of the results obtained for this ligand. The information obtained constitutes additional structural characterization data and is also useful to compare with the results obtained for the newly described 3,4-HPOs (**MRB13**, **MRB15** and **MRB16**), in the same experimental conditions. The crystal structures support unequivocally the synthesis of the desired organic molecules, all isolated in enolic forms as hydrochloride salts (Fig. 2). The asymmetric units (asu's) of four crystal structures are identical, revealing only a respective cationic organic molecule (3,4-HPO ligand) and one chloride anion. The asu of **MRB16** comprises an additional crystallization water molecule. The bond distances of the common 3,4-HPO ring are identical between all the four molecules and also comparable to other previously reported [23,42,48,49]. Interestingly, the C3–O2 bond distance is slightly longer in the **MRB15** and **MRB16** molecules [1.336

Table 3Formulae of the 3,4-HPO chelators and the predicted Log *P* values.

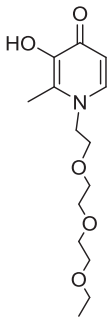
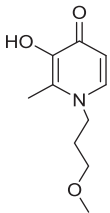
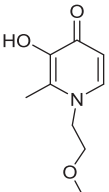
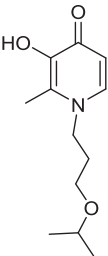
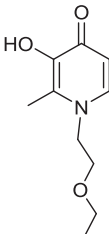
Ligand name	MRB12 [12]	MRB13	MRB14	MRB15	MRB16
Formulae					
Log <i>P</i> (ACD lab)	−0.69	−0.38	−0.50	0.50	0.03

Table 4Geometric information (distances in Å and angles in degrees) for the strong hydrogen bond interactions (D—H...A) of **MRB13**, **MRB14**, **MRB15** and **MRB16**.^a

	D—H...A	<i>d</i> (H...A)	<i>d</i> (D...A)	∠ (DHA)
MRB13	O1—H1...Cl1	2.221(18)	3.029(2)	149(3)
	O2—H2...Cl1 ⁱ	2.071(12)	2.954(2)	169(3)
MRB14	O1—H1...Cl1 ⁱⁱ	2.29(2)	3.037(3)	141(2)
	O2—H2...Cl1	2.092(13)	2.976(3)	177(3)
MRB15	O1—H1...Cl1 ⁱⁱⁱ	2.234(13)	3.0576(14)	154(2)
	O2—H2...Cl1	2.032(10)	2.9336(13)	178(2)
MRB16	O1—H1...O1W	1.765(11)	2.5830(13)	152.5(16)
	O2—H2...Cl1	2.072(9)	2.9602(10)	177.1(15)
	O1W—H1W...O3 ^{iv}	1.906(9)	2.7812(13)	169.3(17)
	O1W—H2W...Cl1 ^v	2.280(9)	3.1722(11)	177.1(14)

^a Symmetry transformation used to generate equivalent atoms: (i) $-x - 2, -y + 1, -z + 1$; (ii) $-x + 1, y - 1/2, -z + 1/2$; (iii) $-x + 1, y - 1/2, -z + 3/2$; (iv) $-x - 1, -y + 1, -z$; (v) $x, -y + 1/2, z - 1/2$.

(2) and 1.335(2) Å, respectively] than that in the **MRB13** [1.328(2) Å] and **MRB14** [1.324(3) Å] structures.

The relative position of the chloride anions strongly influences the crystal packing arrangement in all the compounds, due to distinct O—H...Cl hydrogen bonds established with the respective organic molecules (Fig. 3; see Table 3 for geometric details about the strong hydrogen bonding interactions found in all the structures). In the **MRB13** structure a pair of chloride anions bridges two neighboring organic molecules positioned in anti-parallel mode, by O—H...Cl hydrogen bonds involving the hydroxyl groups in the pyridinone ring, and originating discrete supramolecular species (Fig. 3-MRB13).

In the structures of **MRB14** and **MRB15**, the O—H...Cl hydrogen bonds established between the hydroxyl groups of adjacent molecules and the chloride anions lead to the formation of one-dimensional supramolecular entities (Fig. 3-MRB14 and -MRB15). Both supramolecular chains show a zig-zag arrangement and extend along the *b*-axis of the respective unit cell.

The existence of crystallization water molecules in the structure of **MRB16** besides the chloride anions promotes an extensive hydrogen bonding network (strong O—H...O and O—H...Cl interactions) involving the contiguous organic molecules and leads to the formation of two-dimensional supramolecular structures (supramolecular layers) extended in the [1 0 0] direction of the unit cell (Fig. 3-MRB16). In **MRB16**, contrasting with the remaining compounds where only the hydroxyl groups of the 3-hydroxy-4-pyridinone rings are engaged in the hydrogen bonds, the O-atoms of the ether groups in the chains are also involved.

The extended packing of the supramolecular entities previously described (discrete in **MRB13**, one-dimensional in **MRB14** and **MRB15**, and two-dimensional structures in **MRB16**) is further

reinforced by an extensive network of weak non-covalent interactions, particularly C—H...Cl, C—H...O and C—H... π interactions (not shown; Fig. 4). As consequence of the overall hydrogen bonding network all the compounds reveal stable three-dimensional supramolecular structures with a crystal packing considerably dense.

3.5. Analytical results

3.5.1. Features of the colorimetric determination of iron(III)

The performance of **MRB13**–**MRB16** as colorimetric reagents for iron(III) determination was evaluated using the previously described sequential injection method [12] and compared with preceding results obtained for the parent ligand **MRB12**.

Calibration curves were performed using iron(III) standards in the range 1.8–18 $\mu\text{mol/L}$ (0.10–1.0 mg/L) and the analytical features displayed with the use of each ligand are summarized in Table 5. Data related with results obtained with **MRB12** was also included for comparison.

The sensitivity was set as the calibration curve slope and the limit of detection calculated as the concentration corresponding to 3 times the standard deviation of the blank signal. The precision was evaluated based on the relative standard deviation of the 9.0 $\mu\text{mol/L}$ iron(III) standard.

From analysis of the results summarized in Table 5, we verified that all ligands exhibited a good performance in the determination of iron(III). The results have shown no significant differences in the LOD and precision parameters between the ligands studied in the present work and with the previously tested **MRB12**. Also, no relevant differences were detected in the sensitivity of the method

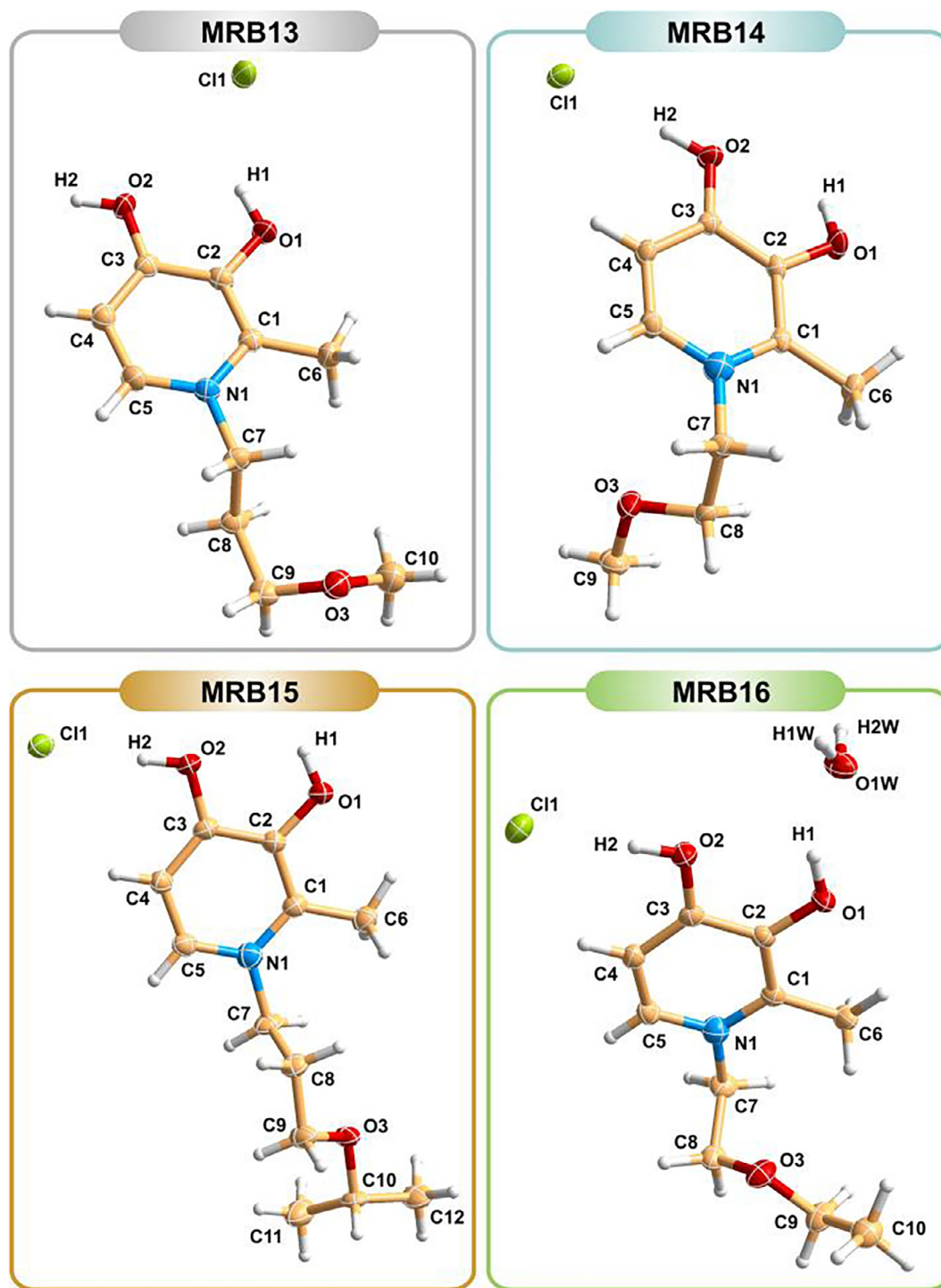


Fig. 2. Crystal structures of the 3,4-HPO molecules (**MRB13**, **MRB14**, **MRB15** and **MRB16**), showing the label scheme for all non-H-atoms which are represented as thermal ellipsoids drawn at the 50% probability level, while H-atoms are shown as small spheres with arbitrary radius.

involving the different ligands comparing to the value determined for **MRB12** (relative deviation, RD <8%).

The results suggest that this new set of 3,4-HPO ligands functionalized with variable ether-derived chains possess a suitable water solubility to guarantee the high sensitivity and low detection limit when compared to the results obtained for the non-ether derived 3,4-HPO, Hmpp, and in a similar mode with that described for **MRB12** [12]. Despite their variable Log *P* values

(−0.69 < Log *P* < 0.50), all the these “ether derived 3,4-HPO ligands” exhibited similar performance in SI method analytical determination of iron(III).

3.5.2. Assessment of potential interferences in water monitoring

Additionally, as previously intended with **MRB12**, the potential application to natural waters requires an effective selectivity in comparison with other ions possibly present. In this context the

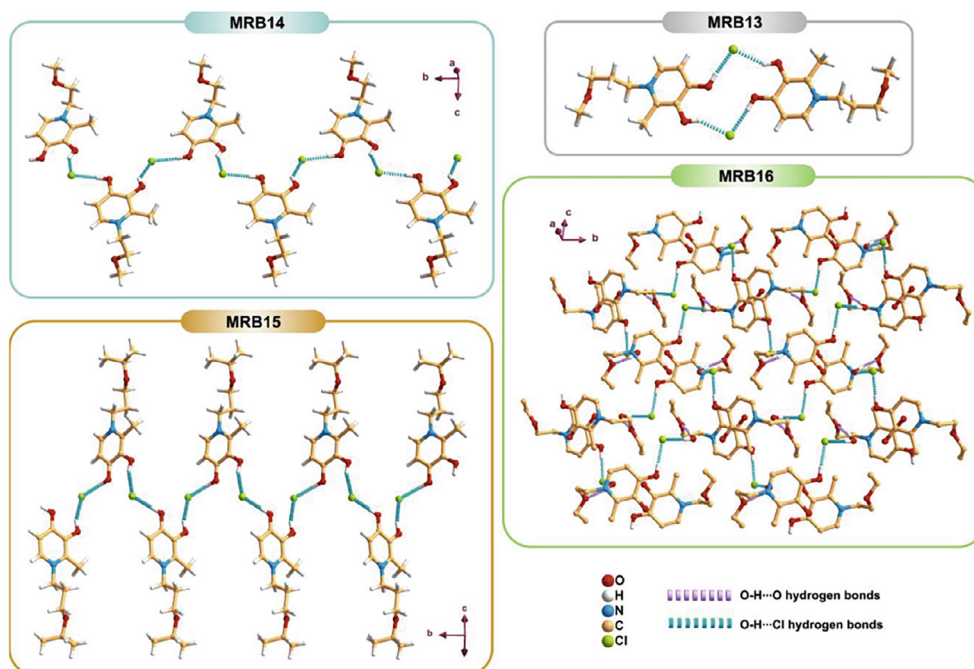


Fig. 3. O—H...Cl (blue dashed lines) and O—H...O (lavender dashed lines) hydrogen bond interaction originating discrete (**MRB13**), one-dimensional (**MRB14** and **MRB15**) and two-dimensional (**MRB16**) supramolecular structures. (Color online.)

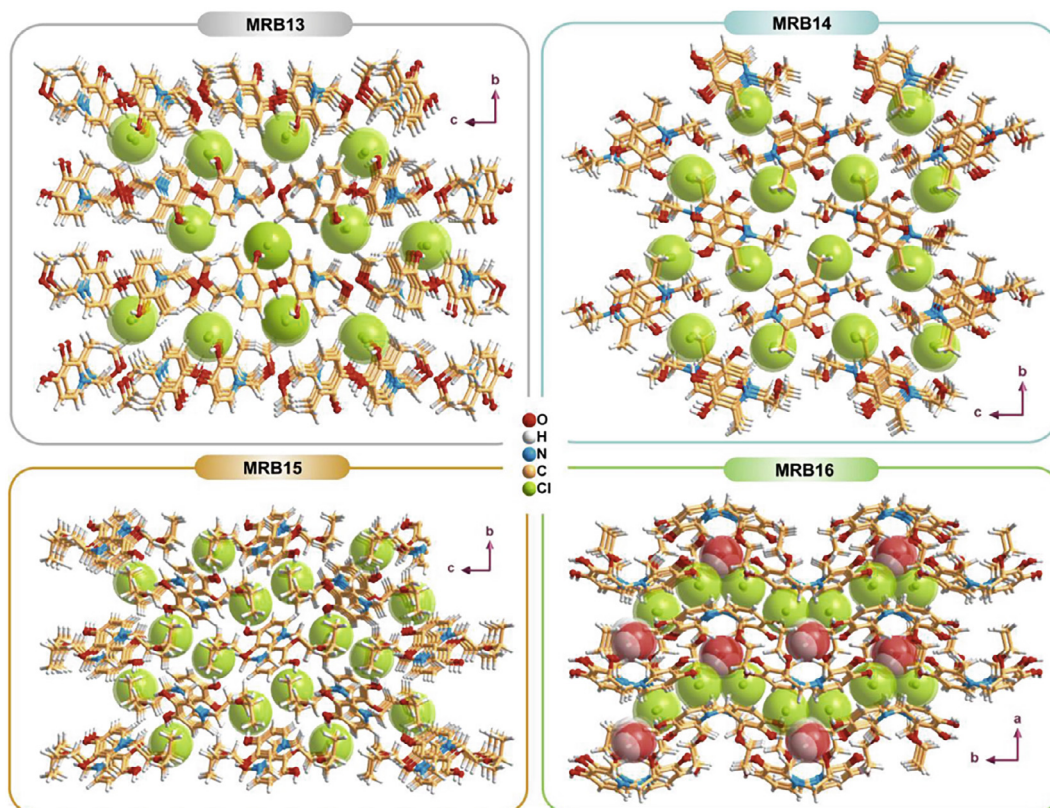


Fig. 4. Extended crystal packing viewed in the [1 0 0] (**MRB13**, **MRB14** and **MRB15**) and [0 0 1] (**MRB16**) direction of the respective unit cell, with the charge balancing chloride anions and crystallization water molecules (only in **MRB16**) drawn in space-filling model.

assessment of potential interferences was carried out, based upon the expected values in natural waters, defined by UNFAO (United Nations Food and Agriculture Organization) [50]. The percentage

of interference (IP) was calculated comparing the analytical signal obtained for an iron(III) standard with a mixed standard of iron(III) and the potential interfering ion. Experiments were performed

Table 5
Analytical features of the methods using different ligands for iron(III) determination considering the previously described SI method [12]. LOD – Limit of detection; RSD – Relative standard deviation.

Ligand	Ligand concentration of 0.6 mmol/L (g/L)	Sensitivity: calibration curve slope (L/mmol)	LOD ($\mu\text{mol/L}$)	Precision: RSD (%), $[\text{Fe}^{3+}] = 9.0 \mu\text{mol/L}$
MRB12 [12]	0.193	$s = 12.8 \pm 0.4$	1.27	1
MRB13	0.140	$s = 13.0 \pm 0.9$	1.24	1
MRB14	0.131	$s = 13.6 \pm 0.7$	1.40	1
MRB15	0.157	$s = 13.8 \pm 0.5$	1.74	1
MRB16	0.140	$s = 13.7 \pm 0.8$	1.79	2

Table 6
Assessment of the influence of potential interfering ions (M^{n+}), for the five ligands, using the developed μSIA method, using an iron standard of 0.50 mg/L (8.95 $\mu\text{mol/L}$); values with bold numbers represent the maximum ratio without significant interference (<10%).

Potential interfering ion (M^{n+})	UNFAO limits (mg/L)	$[\text{M}^{n+}]$ (mg/L)	IP (%)				
			MRB12	MRB13	MRB14	MRB15	MRB16
Al^{3+}	5	5	–5	–2	–	–8	–3
		10	–8	–14	<10	–	–
Ca^{2+}	15	15	–0.5	0.3	–	2	0.9
		30	11	16	<10	12	–21
Co^{2+}	0.1	0.1	2	–0.5	–	5	6
		0.3	11	20	3	12	–21
Mg^{2+}	5	20	2	1	0.1	5	–
		40	24	21	24	16	–1
Mn^{2+}	0.2	20	5	4	7	1	–
		30	15	15	23	13	2
Ni^{2+}	0.2	2	5	–	–	–	–4
		5	13	<10	<10	7	10
Zn^{2+}	2	10	1	–5	1	–3	–
		30	12	13	15	15	<10
Cu^{2+}	1.3	5	5	2	–	4	–
		10	13	12	<10	16	<10
Cd^{2+}	–	0.1	4	1	–	–	–
		0.5	17	14	5	2	<10
Pb^{2+}	–	0.1	3	–	–	0.5	–
		0.5	14	–0.2	4	10	5
Cr^{3+}	–	0.05	7	–	–	–	–
		0.1	13	–2	2	<10	<10

using concentrations of the potential interfering metal ion (M^{n+}) identical or greater than the UNFAO value. The standards were prepared with 0.50 mg/L (8.95 $\mu\text{mol/L}$) of iron(III) and with or without interfering ion. The tested interfering ions, with respective concentrations and the interference percentages are presented in Table 6.

The results shown in Table 6 are indicative that no significant interferences are expected from metal ions existent in natural waters. All the ligands tolerate the interference in quantities greater than the limits defined.

4. Conclusions

We report the synthesis and structural characterization of three novel 3,4-HPO chelators with different ether derived substituents in the nitrogen atom of the heterocyclic ring. The three compounds, together with one previously described and revisited in this study, provide a range of Log P values between $-0.69 < \text{Log } P < 0.50$. Chelators were successfully obtained in high reaction yields by microwave-assisted methods and using commercially available amines as precursors. All the ligands were obtained in an easier, quicker, and more efficient and sustainable way in comparison with the methods described for the synthesis of a highly water soluble 3,4-HPO chelator, **MRB12** [12]. The reduction of overall reaction times, the reproducibility of the experiments and the lower number of steps, constitutes a great advantage considering the need of these ligands as well as their respective metal ion complexes, to be used in many analytical, biological and agricultural applications.

In order to evaluate the potential of the new compounds as analytical reagents in iron(III) determination by sequential injection methods, we tested **MRB13–MRB16** ligands in the same conditions used for **MRB12**. Results showed that all the ligands described are promising molecules for this assay since they exhibit similar results, highlighting the fact that the structural differences introduced do not compromise their performance in iron(III) determination in aqueous samples. Also, results regarding the relevance of several metal ions as potential interferences reinforce the potential application of the ligands in natural water monitoring.

In summary, the new procedure is advantageous to obtain highly water soluble compounds that suitable for analytical applications like metal ion determination [11,12,30], biological purposes, such as the treatment of several diseases like Iron Overload [51–53], Diabetes [54–56] and in agriculture to address Plant Iron Deficiency Chlorosis [17,57–59].

Acknowledgments

This work received financial support from the European Union (FEDER funds through COMPETE) and National Funds (FCT, Fundação para a Ciência e Tecnologia), under the Partnership Agreement PT2020 through project UID/QUI/50006/2013-POCI/01/0145/FEDER/007265 (LAQV/REQUIMTE) and PTDC/AGRPRO/3515/2014-POCI-01-0145-FEDER-016599. Programa Operacional Regional do Norte (ON.2 – O Novo Norte), under the Quadro de Referência Estratégico Nacional (QREN) and funded by Fundo Europeu de Desenvolvimento Regional (Feder) NORTE-07-0124-

FEDER-000066 and NORTE-01-0145-FEDER-000024. R.B.R. Mesquita thanks for the grant SFRH/BDP/112032/2015. The Bruker Avance III 400 spectrometer is part of the National NMR network and was purchased under the framework of the National Programme for Scientific Re-equipment, contract REDE/1517/RMN/2005, with funds from POCI 2010 (FEDER) and (FCT).

Appendix A. Supplementary data

CCDC 1845145, 1845146, 1845147 and 1845148 contains the supplementary crystallographic data for **MRB13**, **MRB14**, **MRB15** and **MRB16**. These data can be obtained free of charge via <http://www.ccdc.cam.ac.uk/conts/retrieving.html>, or from the Cambridge Crystallographic Data Centre, 12 Union Road, Cambridge CB2 1EZ, UK; fax: (+44) 1223-336-033; or e-mail: deposit@ccdc.cam.ac.uk. Supplementary data to this article can be found online at <https://doi.org/10.1016/j.poly.2018.12.005>.

References

- [1] M.A. Santos, S.M. Marques, S. Chaves, Hydroxypyridinones as “privileged” chelating structures for the design of medicinal drugs, *Coord. Chem. Rev.* 256 (2012) 240.
- [2] R. Grazina, L. Gano, J. Sebestik, M. Amelia, New tripodal hydroxypyridinone based chelating agents for Fe(III), Al(III) and Ga(III): Synthesis, physico-chemical properties and bioevaluation, *J. Inorg. Biochem.* 103 (2009) 262.
- [3] T. Zhou, Y. Ma, X. Kong, R.C. Hider, Design of iron chelators with therapeutic application, *Dalton Trans.* 41 (2012) 6371.
- [4] R. Cusnir, C. Imberti, R.C. Hider, P.J. Blower, M.T. Ma, Hydroxypyridinone chelators: from iron scavenging to radiopharmaceuticals for PET imaging with gallium-68, *Int. J. Mol. Sci.* 18 (2017) 1.
- [5] Z.D. Liu, R.C. Hider, Design of iron chelators with therapeutic application, *Coord. Chem. Rev.* 232 (2002) 151.
- [6] Z.D. Liu, R.C. Hider, Design of clinically useful iron(III)-selective chelators, *Med. Res. Rev.* 22 (2002) 26.
- [7] T. Zhou, G. Winkelmann, Z.-Y. Dai, R.C. Hider, Design of clinically useful macromolecular iron chelators, *J. Pharm. Pharmacol.* 63 (2011) 893.
- [8] R.C. Hider, S. Roy, Y.M. Ma, X. Le Kong, J. Preston, The potential application of iron chelators for the treatment of neurodegenerative diseases, *Metallomics* 3 (2011) 239.
- [9] S. Chaves, L. Piemontese, A. Hiremathad, M.A. Santos, Hydroxypyridinone derivatives: a fascinating class of chelators with therapeutic applications - An update, *Curr. Med. Chem.* 25 (2018) 97.
- [10] R.C. Chisté, D. Ribeiro, M. Freitas, A. Leite, T. Moniz, M. Rangel, E. Fernandes, Uncovering novel 3-hydroxy-4-pyridinone metal ion complexes with potential anti-inflammatory properties, *J. Inorg. Biochem.* 155 (2016) 9.
- [11] A. González, R.B.R. Mesquita, J. Avivar, T. Moniz, M. Rangel, V. Cerdà, A.O.S.S. Rangel, Microsequential injection lab-on-valve system for the spectrophotometric bi-parametric determination of iron and copper in natural waters, *Talanta* 167 (2017) 703.
- [12] R.B.R. Mesquita, T. Moniz, J.L.A. Miranda, V. Gomes, A.M.N. Silva, J.E. Rodriguez-Borges, A.O.S.S. Rangel, M. Rangel, Synthesis and characterization of a 3-hydroxy-4-pyridinone chelator functionalized with a polyethylene glycol (PEG) chain aimed at sequential injection determination of iron in natural waters, *Polyhedron* 101 (2015) 171.
- [13] T. Moniz, M.J. Amorim, R. Ferreira, A. Nunes, A. Silva, C. Queirós, A. Leite, P. Gameiro, B. Sarmento, F. Remião, Y. Yoshikawa, H. Sakurai, M. Rangel, Investigation of the insulin-like properties of zinc(II) complexes of 3-hydroxy-4-pyridinones: Identification of a compound with glucose lowering effect in STZ-induced type I diabetic animals, *J. Inorg. Biochem.* 105 (2011) 1675.
- [14] T. Moniz, A. Nunes, A.M.G. Silva, C. Queirós, G. Ivanova, M.S. Gomes, M. Rangel, Rhodamine labeling of 3-hydroxy-4-pyridinone iron chelators is an important contribution to target *Mycobacterium avium* infection, *J. Inorg. Biochem.* 121 (2013) 156.
- [15] T. Moniz, C. Queirós, R. Ferreira, A. Leite, P. Gameiro, A.M.G. Silva, M. Rangel, Design of a water soluble 1,8-naphthalimide/3-hydroxy-4-pyridinone conjugate: investigation of its spectroscopic properties at variable pH and in the presence of Fe³⁺, Cu²⁺ and Zn²⁺, *Dyes Pigm.* 98 (2013) 201.
- [16] T. Moniz, D. Silva, T. Silva, M.S. Gomes, M. Rangel, Antimycobacterial activity of rhodamine 3,4-HPO iron chelators against *Mycobacterium avium*: analysis of the contribution of functional groups and of chelator's combination with ethambutol, *MedChemComm* 6 (2015) 2194.
- [17] C.S. Santos, S.M.P. Carvalho, A. Leite, T. Moniz, M. Roriz, A.O.S.S. Rangel, M. Rangel, M.W. Vasconcelos, Effect of tris(3-hydroxy-4-pyridinone) iron(III) complexes on iron uptake and storage in soybean (*Glycine max* L.), *Plant Physiol. Biochem.* 106 (2016) 91.
- [18] J. Burgess, B. DeCastro, C. Oliveira, M. Rangel, W. Schlindwein, Synthesis and characterization of 3-hydroxy-4-pyridinone-oxovanadium(IV) complexes, *Polyhedron* 16 (1997) 789.
- [19] P.S. Dobbin, R.C. Hider, A.D. Hall, P.D. Taylor, P. Sarpong, J.B. Porter, G.Y. Xiao, D. Vanderhelm, Synthesis, physicochemical properties, and biological evaluation of n-substituted 2-alkyl-3-hydroxy-4(1H)-pyridinones - orally-active iron chelators with clinical potential, *J. Med. Chem.* 36 (1993) 2448.
- [20] R.C. Scarrow, P.E. Riley, K. Abudari, D.L. White, K.N. Raymond, Ferric ion sequestering agents.13. Synthesis, structures, and thermodynamics of complexation of cobalt(III) and iron(III) Tris complexes of several chelating hydroxypyridinones, *Inorg. Chem.* 24 (1985) 954.
- [21] M.A. Santos, M. Gil, L. Gano, S. Chaves, Bifunctional 3-hydroxy-4-pyridinone derivatives as potential pharmaceuticals: synthesis, complexation with Fe(III), Al(III) and Ga(III) and in vivo evaluation with Ga-67, *J. Biol. Inorg. Chem.* 10 (2005) 564.
- [22] S. Fakih, M. Podinovskaia, X. Kong, H.L. Collins, U.E. Schaible, R.C. Hider, Targeting the lysosome: fluorescent iron(III) chelators to selectively monitor endosomal/lysosomal labile iron pools, *J. Med. Chem.* 51 (2008) 4539.
- [23] A.M.G. Silva, A. Leite, M. Andrade, P. Gameiro, P. Brandão, V. Felix, B. de Castro, M. Rangel, Microwave-assisted synthesis of 3-hydroxy-4-pyridinone/naphthalene conjugates. Structural characterization and selection of a fluorescent ion sensor, *Tetrahedron* 66 (2010) 8544.
- [24] S. Battah, R.C. Hider, A.J. MacRobert, P.S. Dobbin, T. Zhou, Hydroxypyridinone and 5-aminolaevulinic acid conjugates for photodynamic therapy, *J. Med. Chem.* 60 (2017) 3498.
- [25] C.F. Zhu, S. Battah, X. Kong, B.J. Reeder, R.C. Hider, T. Zhou, Design, synthesis and biological evaluation of 5-aminolaevulinic acid/3-hydroxypyridinone conjugates as potential photodynamic therapeutical agents, *Bioorg. Med. Chem. Lett.* 25 (2015) 558.
- [26] D.F. Li, P.P. Hu, M.S. Liu, X.L. Kong, J.C. Zhang, R.C. Hider, T. Zhou, Design and synthesis of hydroxypyridinone-L-phenylalanine conjugates as potential tyrosinase inhibitors, *J. Agric. Food Chem.* 61 (2013) 6597.
- [27] G. Liu, F.W. Bruenger, S.C. Miller, A.M. Arif, Molecular structure and biological and pharmacological properties of 3-hydroxy-2-methyl-1-(β-D-ribofuranosyl or pyranosyl)-4-pyridinone: potential iron overload drugs for oral administration, *Bioorg. Med. Chem. Lett.* 8 (1998) 3077.
- [28] Z.M.A.M. Balcerzak, Separation, Preconcentration and Spectrophotometry in Inorganic Analysis, First Ed., Elsevier, Netherlands, 2000.
- [29] R. Suárez, R.B.R. Mesquita, M. Rangel, V. Cerdà, A.O.S.S. Rangel, Iron speciation by microsequential injection solid phase spectrometry using 3-hydroxy-1(H)-2-methyl-4-pyridinone as chromogenic reagent, *Talanta* 133 (2015) 15.
- [30] R.B. Mesquita, R. Suarez, V. Cerdà, M. Rangel, A.O. Rangel, Exploiting the use of 3,4-HPO ligands as nontoxic reagents for the determination of iron in natural waters with a sequential injection approach, *Talanta* 108 (2013) 38.
- [31] Z. Zhang, S.J. Rettig, C. Orvig, Lipophilic coordination compounds: aluminum, gallium, and indium complexes of 1-aryl-3-hydroxy-2-methyl-4-pyridinones, *Inorg. Chem.* 30 (1991) 509.
- [32] T. Kottke, D. Stalke, Crystal handling at low temperatures, *J. Appl. Crystallogr.* 26 (1993) 615.
- [33] apex2, Data Collection Software Version 2012.4, Bruker AXS, Delft, The Netherlands, 2012.
- [34] Cryopad, Remote monitoring and control, Version 1.451, Oxford Cryosystems, Oxford, United Kingdom, 2006.
- [35] saint+, Data Integration Engine v. 8.27b©, 1997–2012, Bruker AXS, Madison, Wisconsin, USA.
- [36] G.M. Sheldrick, SADABS 2012/1, Bruker AXS Area Detector Scaling and Absorption Correction Program, 2012, Bruker AXS, Madison, Wisconsin, USA, 2012.
- [37] G.M. Sheldrick, A short history of SHELX, *Acta Crystallogr., Sect. A* 64 (2008) 112.
- [38] G.M. Sheldrick, SHELXL v. 2014/3, Program for Crystal Structure Refinement, University of Göttingen, 2014.
- [39] G.M. Sheldrick, SHELXT-2014, Program for Crystal Structure Solution, University of Göttingen, 2014.
- [40] C. Queiros, M.J. Amorim, A. Leite, M. Ferreira, P. Gameiro, B. de Castro, K. Biernacki, A. Magalhães, J. Burgess, M. Rangel, Nickel(II) and cobalt(II) 3-hydroxy-4-pyridinone complexes: synthesis, characterization and speciation studies in aqueous solution, *Eur. J. Inorg. Chem.* 2011 (2011) 131.
- [41] P.S. Dobbin, R.C. Hider, A.D. Hall, P.D. Taylor, P. Sarpong, J.B. Porter, G. Xiao, D. van der Helm, Synthesis, physicochemical properties, and biological evaluation of N-substituted 2-alkyl-3-hydroxy-4(1H)-pyridinones: orally active iron chelators with clinical potential, *J. Med. Chem.* 36 (1993) 2448.
- [42] G. Xiao, D. van der Helm, F.H. Goerlitz, R.C. Hider, P.S. Dobbin, Structures of 3-hydroxy-1-(2-methoxyethyl)-2-methyl-4-pyridinone, its hydrochloride and 1-ethyl-3-hydroxy-2-methyl-4-pyridinone hydrochloride hydrate, *Acta Crystallogr., Sect. C* 49 (Pt 9) (1993) 1646.
- [43] W. Huang, R. Richert, The physics of heating by time-dependent fields: microwaves and water revisited, *J. Phys. Chem. B* 112 (2008) 9909.
- [44] J. Robinson, S. Kingman, D. Irvine, P. Licence, A. Smith, G. Dimitrakis, D. Obermayer, C.O. Kappe, Understanding microwave heating effects in single mode type cavities-theory and experiment, *PCCP* 12 (2010) 4750.
- [45] K.C. Oliver, Controlled microwave heating in modern organic synthesis, *Angew. Chem. Int. Ed.* 43 (2004) 6250.
- [46] acd/LogP Software (assessed 12th April 2017). Available from: <http://www.acdlabs.com/resources/freeware/chemsketch/logp/>.
- [47] T. Moniz, J.T.S. Coimbra, N.F. Bras, L. Cunha-Silva, M.J. Ramos, P.A. Fernandes, B. de Castro, M. Rangel, Synthesis and structural characterization, by spectroscopic and computational methods, of two fluorescent 3-hydroxy-4-pyridinone chelators bearing sulphorhodamine B and naphthalene, *RSC Adv.* 6 (2016) 4200.

- [48] J. Burgess, J. Fawcett, S.A. Parsons, 3-Hydroxy-1-(3-imidazolylpropyl)-2-methyl-4-pyridinone dihydrochloride dihydrate, *Acta Crystallogr., Sect. E* 57 (2001) o1016.
- [49] S. Hall, R. Roy, D. McLaughlin, K. Sullivan, L. Barclay, C. Vogels, A. Decken, S. Westcott, The synthesis and molecular structure of 1-(3,4-dihydroxyphenethyl)-3-hydroxy-2-methylpyridin-4(1H)-one hydrochloride methanol solvate, *Crystals* 3 (2013) 333.
- [50] L.S. Clescerl, A.E. Greenberg, A.D. Eaton, *Standard Methods for the Examination of Water and Wastewater*, Part 3000 Metals, 1999, 20th ed.
- [51] G. Crisponi, M. Remelli, Iron chelating agents for the treatment of iron overload, *Coord. Chem. Rev.* 252 (2008) 1225.
- [52] D.S. Kalinowski, D.R. Richardson, The evolution of iron chelators for the treatment of iron overload disease and cancer, *Pharmacol. Rev.* 57 (2005) 547.
- [53] G.J. Kontoghiorghe, K. Neocleous, A. Kolnagou, Benefits and risks of deferiprone in iron overload in thalassaemia and other conditions, *Drug Saf.* 26 (2003) 553.
- [54] T. Jakusch, T. Kiss, In vitro study of the antidiabetic behavior of vanadium compounds, *Coord. Chem. Rev.* 351 (2017) 118.
- [55] H. Sakurai, Y. Kojima, Y. Yoshikawa, K. Kawabe, H. Yasui, Antidiabetic vanadium(IV) and zinc(II) complexes, *Coord. Chem. Rev.* 226 (2002) 187.
- [56] H. Sakurai, Y. Yoshikawa, H. Yasui, Current state for the development of metallopharmaceutics and anti-diabetic metal complexes, *Chem. Soc. Rev.* 37 (2008) 2383.
- [57] J. Abadía, S. Vázquez, R. Rellán-Álvarez, H. El-Jendoubi, A. Abadía, A. Álvarez-Fernández, A.F. López-Millán, Towards a knowledge-based correction of iron chlorosis, *Plant Physiol. Biochem.* 49 (2011) 471.
- [58] M. Shenker, Y. Chen, Increasing iron availability to crops: fertilizers, organo-fertilizers, and biological approaches, *Soil Sci. Plant Nutr.* 51 (2005) 1.
- [59] J.J. Lucena, Fe chelates for remediation of Fe chlorosis in strategy I plants, *J. Plant Nutr.* 26 (2003) 1969.